

Delocalized Surface Modes Reveal Three-Dimensional Structures of Complex Biomolecules

A. B. Sugiharto, C. M. Johnson, I. E. Dunlop, and S. Roke*

Max Planck Institute for Metals Research, Heisenbergstrasse 3, 70569 Stuttgart, Germany

Received: February 12, 2008; Revised Manuscript Received: April 10, 2008

Interfaces are important for many processes in chemistry, physics, and biology. Crucial to their properties are the details of the three-dimensional structure of the participating (macro)molecules. Vibrational Sum Frequency Generation (VSFG) is a tool specifically suited to probing the first few atomic layers of an interface. Traditionally, interfaces are probed by mapping localized vibrational modes. Here, we show that the three-dimensional structure of large interfacial biomolecules can be probed by measuring delocalized vibrational backbone modes, which appear to be extremely sensitive to changes in the skeletal structure. We demonstrate that for three different films of chemically identical poly(lactic acid) polymer, we can observe dramatic changes in the three-dimensional arrangement of the surface molecular backbones. This type of information could not be obtained from probing only localized group modes.

Introduction

Interfaces are important for many processes in chemistry, physics, and biology. They form the barriers between different media and control numerous processes, such as (e.g.) transport between different media and binding of molecules to receptors. Crucial in those processes are the details of the 3D structure of the participating (macro)molecules. Since the molecules that are present in the first few atomic monolayers away from the interface are—even for very thin films—vastly outnumbered by the bulk molecules, pure interfacial information is difficult to obtain. Here, we show for the first time that we can probe the secondary and tertiary structure of three forms of chemically identical biopolymer molecules situated at the interface by performing Vibrational Sum Frequency Generation (VSFG) on delocalized vibrational modes.

In our VSFG experiment, an infrared (IR) and a visible (VIS) laser pulse are reflected from the interface of a biopolymer film (see the inset to Figure 2). In the first few atomic monolayers of the polymer/air interface, photons are created with the sum of the incoming frequencies. If the IR energy coincides with that of a vibrational resonance, there is an enhanced interaction that enables the vibrational spectroscopy of the first few atomic monolayers away from the interface.^{1a} This interaction originates from a combined IR and Raman process, which occurs only in the noncentrosymmetric (surface) regions. It contains valuable information regarding the structure of interface molecules.

Nowadays, VSFG is widely and successfully employed to probe vibrational modes in the high-frequency region (1500–4000 cm^{-1}) of the IR spectrum.¹ However, these vibrations constitute highly localized modes. Therefore, such measurements mostly report on very local structural parts of the interfacial molecules (i.e., presence and orientation of, e.g., $-\text{CH}_3$, $-\text{OH}$, and $\text{C}=\text{O}$ groups). Recently, developments^{1b–d} have been made to access a wider variety of surface chemical groups, such as the amide

group that allows for the identification of α helices and β sheets (in molecules where amide bonds are present).^{1b} This type of structural information still depends on the presence of a single chemical group. In contrast to high-frequency localized modes, low-frequency (skeletal) modes are often composed of the movement of several chemical groups. Thanks to their delocalized nature, these modes are extremely sensitive to the 3D structure of molecules. Their frequency, intensity, and width can be important markers of the secondary and tertiary structure of proteins, peptides, and other complex (bio)molecules.

We report femtosecond VSFG spectroscopy on such delocalized modes in the fingerprint region for three different films of chemically identical biopolymers [poly(lactic acid) (PLA)]. This polymer is considered to be an environmentally friendly, biodegradable, and biocompatible alternative to many plastics and represents a wide range of macromolecules. Already, it is being developed for diverse purposes such as a packing material,^{2a} a material for implants,^{2b,c} and a medicine carrier.^{2d} Therefore, it is important to understand how the interface is composed and whether it changes if different forms are used. We studied the 3D surface structure of amorphous L-PLA (L-A), crystalline L-PLA (L-C), and racemic D/L-PLA (R).

Experimental Methods

Film Preparation. The PLA films were drop-casted on glass substrates from 2.5 wt% solutions of polymer powder (L-PLA or PLA polymerized from a 1:1 mixture of L-lactide and D-lactide, obtained from Purac Biochem) dissolved in chloroform (>99% Merck). The glass plates were cleaned with a 3:1 aqueous solution of $\text{H}_2\text{SO}_4/\text{H}_2\text{O}_2$ (Sigma-Aldrich) and later rinsed with 18 M Ω cm Millipore water. This procedure generated films of thicknesses of less than 1 μm , as measured by ellipsometry (M-2000 R from J.A. Woollam Co). The resultant L-PLA and D/L-PLA films had a low degree of crystallinity and are referred to as the L-A and R films. To obtain crystalline (L-C) films, the L-A films were annealed at $\sim 120^\circ\text{C}$ for 15 min. The presence (or absence) of spherulites was confirmed

* To whom correspondence should be addressed. E-mail: roke@mf.mpg.de.

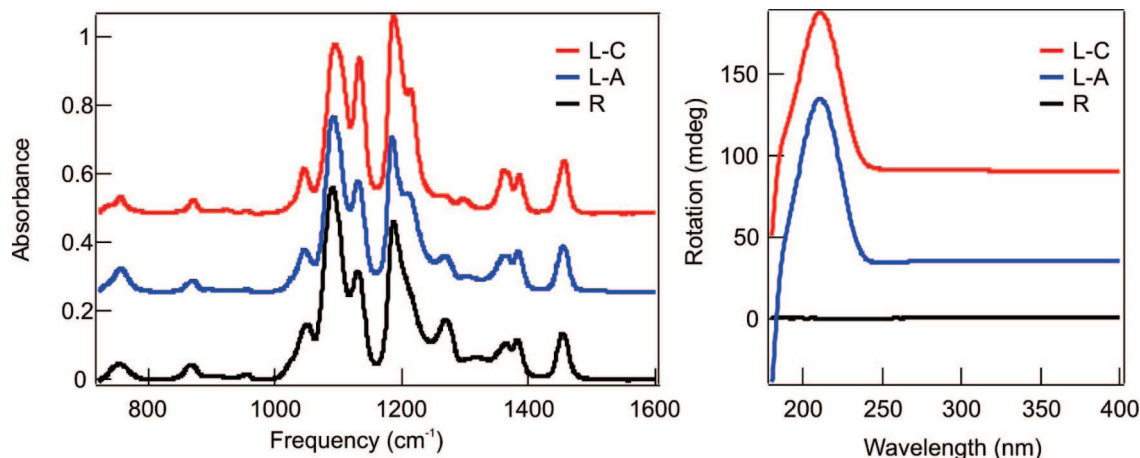


Figure 1. Left: IR spectra (left) and CD measurements (right) of L-crystalline (L-C), L-amorphous (L-A), and racemic (R) PLA films. The IR spectra display the average bulk structure of the films, and since they are chemically identical, only small differences are observed. The CD spectra show that the L-C and L-A films consist of helices, while the R film displays no rotation since it is racemic.

with crossed-polarized microscopy. Images were taken with an Olympus IX71 microscope. IR spectra were recorded with a Bruker Vertex70 FTIR spectrometer, and the Circular Dichrometry (CD) spectra were recorded with a Jasco J-810 dichrometer.

VSFG Experiments. The VSFG experiments were performed using a 1 kHz broad-band high-power Ti:Sapphire laser system. The p-polarized IR pulses (with 5 μ J energy content) had pulse durations of 150–250 fs. The s-polarized visible pulses (with 3 μ J energy content) were centered at 800 nm and shaped to a FWHM of 5 cm^{-1} . The focus diameter was 0.75 mm. Plotted spectra were normalized for pulse energy and acquisition time. The IR and vis beams were incident under 40 and 60° with respect to the surface normal, respectively. This geometry (i.e., incident angles) was chosen such that a maximum signal-to-noise ratio from the polymer/air interface was obtained.

The SFG spectra were recorded with s-polarized SFG and VIS beams and a p-polarized IR beam. This polarization combination only probes the interface of the film and not the bulk,³ even though crystalline L-PLA is a noncentrosymmetric material. The crystallite symmetry belongs to the $P2_12_12_1$ space group,^{4–6} which results in nonzero tensor elements of the bulk second-order susceptibility. They are $\chi^{(2)}_{xyz}$, $\chi^{(2)}_{xzy}$, $\chi^{(2)}_{zyx}$, $\chi^{(2)}_{yxz}$, $\chi^{(2)}_{yzx}$, and $\chi^{(2)}_{yxz}$. For the thin films measured here, these tensor elements will give rise only to signal in the polarization combinations spp, psp, and pps. The polarization combinations ssp, ppp, sps, and pss describe the polymer structure at the interface. For a full description of this behavior, see ref 3.

Results and Discussion

Figure 1 displays infrared (IR) transmission spectra together with CD measurements of the L-C, L-A, and R films. The IR spectra show some changes in the fingerprint region, which are characteristic of the three films.^{3–6} The CD measurements show that the bulk of the L-C and the L-A film is composed of helices.⁷

Figure 2 displays VSFG spectra taken in the vibrational fingerprint region of the same films. The spectra of these three chemically identical films show—in contrast to the IR spectra in Figure 1—a large diversity, which reflects the secondary and tertiary structure of the biopolymer at the interface. Such dramatic changes are not observed in Figure 1 because in linear spectroscopy, all atomic groups in the film participate in generating the signal so that it is the average bulk structure that is compared and not the interfacial one. Direct comparison

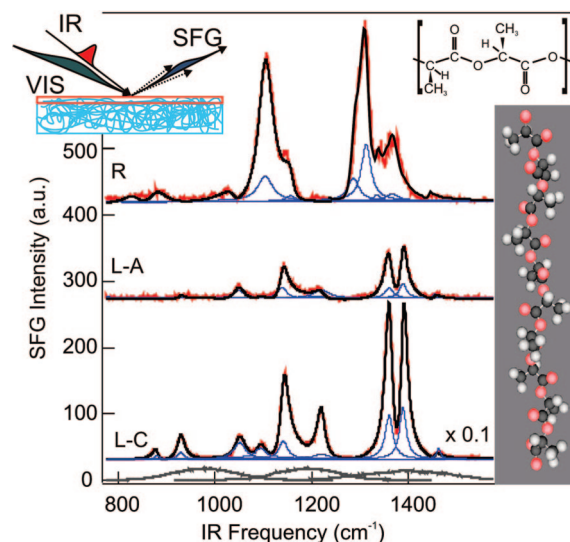


Figure 2. VSFG spectra of the delocalized modes of L-crystalline (L-C), L-amorphous (L-A), and racemic (R) PLA films, taken with three different IR pulses, which are displayed in the bottom. The black lines are fits to the data in which all contributions to the reflected electrical sum frequency field are added. The blue Lorentzians display the most prominent vibrational modes. The chemical repeat unit of L-PLA is also shown, as well as a molecular model of a 10_3 helix. In the top-left panel, the VSFG experiment is illustrated.

between the VSFG spectra and the data in Figure 1 is therefore not very meaningful when it comes to determining the interfacial structure.

The spectra in Figure 2 were fit according to the well-known formula for VSFG (see, e.g., ref 8)

$$I(\omega) \propto \left| \left(A_{\text{NR}} e^{i\Delta\phi} + \sum_n \frac{A_n}{(\omega - \omega_{0n}) - i\Gamma_n} \right) E_{\text{IR}}(\omega) E_{\text{vis}}(\omega) \right|^2 \quad (1)$$

This signal consists of a single non-resonant (frequency-independent) and n resonant electrical field contributions. The resonant contributions are described as damped, exponentially decaying oscillators, with (relative) amplitude A_n , resonance frequency ω_{0n} , and damping constant Γ_n . The frequency-independent non-resonant response has amplitude A_{NR} . The $\Delta\phi$ represents the phase difference between the resonant and non-resonant fields. The spectra were fit using the IR and VIS fields as obtained from measurements. To obtain a wide spectral range, for each film, three different central IR frequencies were used

TABLE 1: Mode Assignments, Resonance Frequencies (ω_{0n}), Relative Amplitudes (A_n), and Spectral Half-Width at Half-Maximum (Γ_n) Used in the Global Fitting Procedures (Parameters Given in the Order L-C/L-A/R)

mode assignment	ω_{0n} (cm ⁻¹)	A_n	Γ_n (cm ⁻¹)
C-COO stretching	-/-/832	-/-/-0.15	-/-/20
C-COO + C-CH ₃ + O-CO stretching	878/878/881	0.22/-0.04/-0.15	6.7/15.5/20
C-CH ₃ rocking + O-CH stretching	929/929/-	0.39/0.02/-	9.2/9.3/-
C-CH ₃ rocking + C-H bending	1051/1049/1050	0.87/0.18/0.02	7.0/12.5/12
C-CH ₃ stretching + C-CH ₃ rocking	1093/1093/1104	0.31/0.04/-0.52	12.7/12.7/18
C-H bending	1141/1139/1157	0.70/0.14/0.14	10.7/10.6/11.3
C-COO + O-CH stretching + C-CH ₃ rocking + C-H bending	1187/-/-	-0.40/-/-	17.1/-/-
C-H bending + O-CH stretching	1216/1220/1216	0.66/-0.07/-0.02	10.6/12.6/20
C-CH ₃ rocking	-/-/1286	-/-/0.37	-/-/14.4
C-H bending	-/-/1312	-/-/-0.48	-/-/11.6
O-CO stretching	1360/1359/1335	1.1/0.17/-0.08	9.2/10.1/6.3
sym. CH ₃ bending	1388/1387/1367	0.96/0.16/0.24	9.6/9.2/16.4
asym. CH ₃ bending	1454/1453/1443	0.22/0.038/0.05	9.0/7.7/6.0

(955, 1181, and 1388 cm⁻¹; see the bottom trace of Figure 2). The obtained spectra were fit using a global fitting procedure, such that the amplitudes, widths, and resonance frequencies of the modes that are present in adjacent spectra were represented by the same fitting parameters. Where possible, literature values of resonant frequencies were used.³⁻⁶

Starting with the L-C spectra, we see clear features that can be assigned to skeletal modes, non-skeletal modes, and combinations of the two. Comparing the resonance frequencies (represented by the blue Lorentzians in the graphs) to previously calculated normal modes for a (10₃) helical geometry and measured IR and Raman spectra of L-PLA, we can determine that the bands observed at 878, 1187, and 1216 cm⁻¹ are delocalized vibrational modes of the helical backbone. The band at 878 cm⁻¹ is a delocalized mode that is spread over the C-COO, the C-CH₃, and the O-CO stretch modes.^{4,5} The mode at 1187 cm⁻¹ is a mode containing components from the C-COO and O-CH stretching modes as well as the CH₃ rocking and C-H bending modes, whereas the band at 1216 cm⁻¹ is composed of C-H bending and O-CH stretching movements. The band at 1093 cm⁻¹ belongs to a slightly more localized combination of a C-CH₃ stretch mode with a C-CH₃ rocking mode,^{5b} and the band at 1360 cm⁻¹ is dominated by the O-CO stretching mode.⁵ Together, these bands form the stretch mode of the helical coil that forms the backbone. Thus, we can for the first time selectively and directly probe the helical motion at the surface. Non-skeletal, more localized modes appear at 929 and 1051 cm⁻¹ (mainly CH₃ rocking), 1141 cm⁻¹ (C-H bending), 1388 cm⁻¹ (sym. CH₃ bending), and 1454 cm⁻¹ (asym. CH₃ bending).^{4,5}

The L-A film displays, for IR frequencies above 1300 cm⁻¹, the same modes, albeit, compared with the L-C film, with different intensities. This difference reflects the disordered nature of the L-A film, resulting in less coherent addition of SFG photons originating from relatively localized modes. At lower frequencies, the modes are more delocalized and thus show a more sensitive behavior toward the 3D structure. The modes at 878, 1187, 929, and 1093 cm⁻¹ are virtually absent. The relative intensities of the C-H bending mode (1139 cm⁻¹), the skeletal combination mode at 1220 cm⁻¹, and the O-CO at stretching modes 1359 cm⁻¹ have not changed significantly. Thus, the surface chains of the L-A film may have a skeletal structure that is similar to those on the surface of the L-C film, just like that in the bulk of the films (see Figure 1). The packing and orientation, however, are significantly different, as witnessed by changes in the rocking modes (at 929, 1051, and 1093 cm⁻¹), which are more sensitive to the environment. The absence of

some of the delocalized backbone modes may indicate a distortion of the skeletal geometry, but since the other skeletal modes have not changed their frequencies, the chains are probably helically shaped.

Comparing these L-C and L-A spectra to the surface spectrum of the R film, we observe a dramatic difference. As can be seen from Figure 2, the modes at 929 cm⁻¹, (CH₃ rocking) and 1220 cm⁻¹ (delocalized skeletal mode) are absent. Shifts appear in the C-CH₃ stretch modes (from 1093 to 1104 cm⁻¹), the C-H bending mode (from 1141 to 1157 cm⁻¹), and the C-COO stretch mode (from 878 to 881 cm⁻¹). Furthermore, new bands appear at 832, 1286, 1312, and 1335 cm⁻¹. Interestingly, the mode at 832 cm⁻¹ coincides with the C-C stretch frequency of an unbound carboxylic acid group.⁴ On the other hand, the mode at 1286 cm⁻¹ has never been reported for racemic PLA^{4,9} but has been calculated to be typical of a 10₃ helical structure.^{5a} It is clear from these large differences that the chain geometry at the surface of the R polymer film is totally different from that of the L-A and L-C films. Also, it is probably a very heterogeneous structure since certain aspects of helicity prevail while at the same time modes appear that are indicative of a more loosely connected monomer-like structure. Table 1 summarizes the above assignments.

Thus, VSFG experiments in the fingerprint region are extremely sensitive to changes of the backbone structure of the outermost polymer monolayer at the polymer/air surface. This previously largely unexplored frequency region allows one to determine whether the interfacial biopolymers are ordered helices (L-C interface), disordered helices (L-A interface), or rather consist of heterogeneously composed chains (R interface).

Figure 3 shows VSFG spectra of the three different films in the high-frequency region. It demonstrates the difference between probing localized and delocalized modes. The R and L-A spectra are dominated by the two modes at 2947 and 2997 cm⁻¹, which correspond to the (localized) symmetrical and antisymmetrical stretch modes of the CH₃ groups. The identical peak positions for two films with such a completely different 3D structure illustrate the added value of mapping low-frequency delocalized modes rather than high-frequency localized ones. The L-C spectrum was fit with two additional peaks, namely, at 2965 and 3007 cm⁻¹, which are needed to account for crystal field splitting.³⁻⁵ As can be seen, the main difference between these spectra is in the intensities rather than in the spectral shapes. Although such an intensity difference already demonstrates the advantage of VSFG over linear vibrational spectroscopy,³ it only reflects the difference in surface order (a consequence of the coherent nature of VSFG). Direct insight

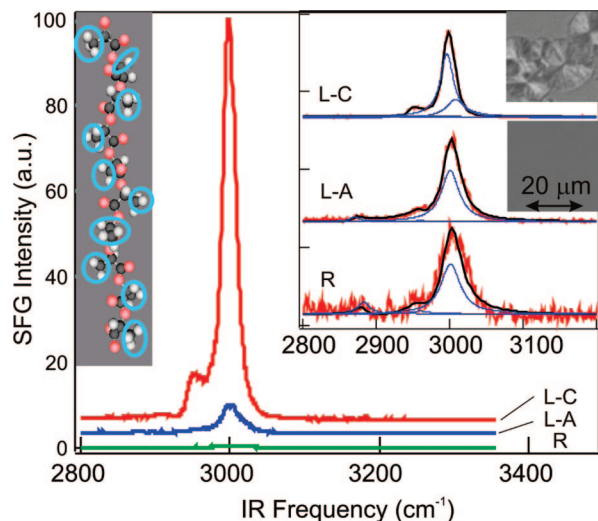


Figure 3. VSFG spectra of L-crystalline (L-C), L-amorphous (L-A), and racemic (R) PLA films, probing the localized methyl stretch modes. The inset shows the scaled spectra together with the fits (black lines). The blue Lorentzians display the vibrational modes. Crossed-polarized microscopy images of the L-C and L-A films reflect the difference in the state of the films. The image of the R film was featureless (just like the one from the L-A film) and has therefore been omitted.

into the 3D arrangement of the biopolymer cannot be obtained. The limited amount of knowledge obtainable from probing localized surface modes with VSFG contrasts starkly with the wealth of information available if one probes delocalized (fingerprint) modes. Still, more information would be accessible if such measurements were combined with a normal-mode analysis.

Conclusions

In summary, we have found that probing the interface of three forms of chemically identical biopolymers in the fingerprint region by VSFG reveals enormous differences in the 3D structure of the complex chains. By probing vibrational modes

that are delocalized over a number of groups on a single chain, one is extremely sensitive to secondary and tertiary structural elements. This ability to follow in detail 3D structures of large (bio)molecules at interfaces should be of enormous value in many fields of research.

Acknowledgment. This work is part of the research program of the Max Planck Society. C.M.J and I.E.D. acknowledge support from the Alexander von Humboldt foundation. We thank R. Fiammengio and R. P. Richter for helpful discussions, A. Batenburg and L. Jeurgens for ellipsometry measurements, and A. Kros for circular dichrometry measurements.

References and Notes

- (1) (a) Shen, Y. R. *Nature* **1989**, 337, 519–525. (b) Chen, X. Y.; Wang, J.; Sniadecki, J. J.; Even, M. A.; Chen, Z. *Langmuir* **2005**, 21, 2662–2664. (c) Ma, G.; Allen, H. C. *Langmuir* **2006**, 22, 5341–5349. (d) Kim, J.; Somorjai, G. A. *J. Am. Chem. Soc.* **2003**, 125, 3150–3158. (e) Chen, Z.; Shen, Y. R.; Somorjai, G. A. *Annu. Rev. Phys. Chem.* **2002**, 53, 437–465.
- (2) (a) Tsuji, H. *Macromol. Biosci.* **2005**, 5, 569–597. (b) Griffith, L. G.; Naughton, G. *Science* **2002**, 295, 1009–1014. (c) Spenlehauer, G. M.; Vert, M.; Benoit, J. P.; Boddaert, A. *Biomaterials* **1989**, 10, 557–563. (d) Nijsen, J. F. W.; Zonnenberg, B. A.; Woittiez, J. R. W.; Rook, D. W.; Swildens-van Woudenberg, I. A.; van Rijk, P. P.; van het Schip, A. D. *Eur. J. Nucl. Med.* **1999**, 26699–26704.
- (3) Johnson, C. M.; Sugiharto, A. B.; Roke, S. *Chem. Phys. Lett.* **2007**, 449, 191–195.
- (4) (a) Cassanas, G.; Morssli, M.; Fabregue, E.; Bardet, L. *J. Raman Spectrosc.* **1991**, 22, 409–413. (b) Cassanas, G.; Kister, G.; Fabregue, E.; Morssli, M.; Bardet, L. *Spectrochim. Acta, Part A* **1993**, 49, 271–279.
- (5) (a) Aou, K.; Hsu, S. L. *Macromolecules* **2006**, 39, 3337–3344. (b) Kang, S. H.; Hsu, S. L.; Stidham, H. D.; Smith, P. B.; Yang, X. Z. *Macromolecule* **2001**, 34, 4542–4548.
- (6) Zhang, J. M.; Sato, H.; Tsuji, H.; Noda, I.; Ozaki, Y. *Macromolecules* **2005**, 38, 1822–1828.
- (7) Kimura, T.; Fukuda, T.; Shimada, S.; Matsuda, H. *Chem. Lett.* **2004**, 33, 608–609.
- (8) (a) Hunt, J. H.; Guyot-Sionnest, P.; Shen, Y. R. *Chem. Phys. Lett.* **1987**, 133, 189–192. (b) Guyot-Sionnest, P.; Hunt, J. H.; Shen, Y. R. *Phys. Rev. Lett.* **1987**, 59, 1597–1600. (c) Lambert, A. G.; Neivandt, D. J.; Briggs, A. M.; Usadi, E. W.; Davies, P. B. *J. Phys. Chem. B* **2002**, 106, 5461–5469.
- (9) Kister, G.; Cassanas, G.; Vert, M. *Polymer* **1998**, 39, 267–273.

JP801254Y